New Precision Measurement of the ^{3}He(^{4}He, γ) ^{7}Be Cross Section

B. S. Nara Singh,[1] M. Hass,[1] Y. Nir-El,[2] and G. Haquin[2]

[1]*Department of Particle Physics, Weizmann Institute of Science, Rehovot, Israel*
[2]*Soreq Research Centre, Yavne, Israel*

The ^{3}He(^{4}He, γ) ^{7}Be reaction plays an important role in determining the high energy solar neutrino flux and in understanding the abundances of primordial ^{7}Li. This Letter reports a new precision measurement of the cross sections of this direct capture reaction, determined by measuring the ensuing ^{7}Be activity in the region of $E_{c.m.} = 420$ to 950 keV. Various recent theoretical fits to our data result in a consistent extrapolated value of $S_{34}(0) = 0.53(2)(1)$ keV b.

PACS numbers: 25.40.Lw, 26.20.+f, 26.65.+t

The ^{3}He(^{4}He, γ) ^{7}Be reaction is one of the remaining major sources of uncertainty [1,2] in determining the high energy solar neutrino flux [3,4] that results from the ^{7}Be(p, γ) ^{8}B reaction [5–7]. It also plays an important role in understanding the primordial ^{7}Li abundance [8,9]. The available data on the astrophysical S factor S_{34} are obtained by using two different methods: the detection of prompt γ rays [10–15] from ^{7}Be or of the ensuing γ activity from ^{7}Be [10,11,16,17]. These two sets of results show a significant scatter and a persistent discrepancy [18,19]. The standard solar model (SSM) calculations [1,2] and standard big bang nucleosynthesis (SBBN) [20] use 0.53(5) keV b of Ref. [18] and 0.54(9) keV b of Ref. [19], respectively, for $S_{34}(0)$. The most recent R-matrix analysis [21] quotes a value of 0.51(4) keV b. A more accurate measurement is therefore highly desirable and recommended [2]. However, no such attempt was made for almost two decades. We have initiated a ^{7}Be activity precision measurement of this cross section at energies around $E_{c.m.} = 420$–950 keV using a ^{3}He beam and a ^{4}He gas target with a Ni-foil window. The focus of the present measurement is to obtain accurate data points at medium energies in order to set the absolute scale of the cross section and for a comparison to previous measurements.

A schematic diagram of our experimental setup is shown in Fig. 1. A ^{3}He beam at $E_{lab} = 1000$ to 2300 keV from the 3 MV Van de Graaff accelerator at the Weizmann Institute enters a ^{4}He gas cell through a 8 mm diameter nickel window of 0.5 to 1 μm thickness. The beam direction is defined by an upstream slit at 2 m from the center of the cell and two Ta collimators of 3 mm, one at the entrance and the other at the exit of the chamber. The beam on target is restricted to be below 1 μA current and is raster scanned over a rectangular area of 3×5 mm^2 in order to avoid excessive localized heating of the Ni window. The gas cell is insulated from the beam line and the entire chamber, including a Cu catcher of 50 mm diameter that is in electric contact with the gas cell, serves as a Faraday cup. The catcher is mounted on a movable arm that allows one to

accurately fix the distance between the Ni foil and the Cu catcher, i.e., the target length. An aperture placed before the Ni window, including a 4 mm Ta collimator, serves as a secondary electron suppressor (Fig. 1) at -400 V that was set by measuring the beam current on the chamber as a function of voltage; there was no discernible variation in beam current upon introducing gas into the chamber. The elastically scattered-beam particles from the Ni window were monitored online using a narrowly collimated Si surface barrier detector placed at an angle of $\theta = 44.7°$. The Ta collimators constrain the beam direction to coincide with the chamber axis and thus determine θ. The number of ^{4}He target atoms per cm^2 is given by $N_t = 9.66 \times 10^{18} l \frac{P}{T_0 + T_c}$ where P, T_0, T_c, and l are gas pressure, room temperature, correction in temperature due to the beam heating and target length given in units of torr, K, and cm, respectively [11,22]. For the typical 500 nA current at the 2 MeV beam we have estimated a value of $\approx$ 17 K for T_c that was confirmed using the 1.518 MeV resonance in the ^{10}B(α, p) ^{13}C reaction. The pressure reading, calibrated to 0.5% by Israel Standard Instruments, and the beam current were monitored to maintain constant values for P and T_c. The ^{4}He purity of 99.9% was ensured by replacing it periodically every four hours. Residual gas leaks resulted in $\sim$0.2 torr increase in the duration of 12 h when $P \gtrsim 20$ torr. This yields an upper limit of 0.3%/4 h
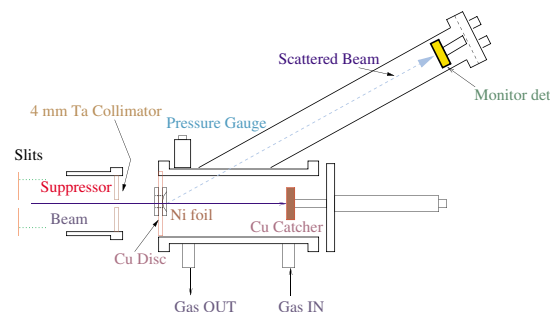

FIG. 1 (color online). A schematic diagram of the experimental setup.

air leak, introducing ~ 1 keV uncertainty in $E_{\text{c.m.}}$ [Eq. (1)]. The beam energy was calibrated using the $^{27}\text{Al}(p, \gamma)^{28}\text{Si}$ resonances at proton energies of 1118.4, 991.2, and 773.7 keV using H_2 and H_3 beams, respectively, in order to correspond to the range of ^3He lab energies and magnetic rigidity. The energy losses and energy straggling of the ^3He beam in the Ni foil (ΔE_{Ni}) and in the ^4He gas (ΔE_{He}) were determined using TRIM [23] and were also checked using the 1.518 MeV resonance in the $^{10}\text{B}(\alpha, p)^{13}\text{C}$ reaction (see below). The center of mass energy for ^3He at the center of the ^4He gas is given by

$$E_{\text{c.m.}} = \frac{4}{7}\left(E_b - \Delta E_{\text{Ni}} - \frac{\Delta E_{\text{He}}}{2}\right), \quad (1)$$

where E_b is the beam energy. In the present energy range, the backscattering loss of the implanted nuclei is not relevant [24]. For a target of finite energy width (ΔE_T), the measured cross sections are expressed as a function of the effective energies, $\overline{E}_{\text{c.m.}}$ obtained by a treatment similar to Ref. [6]. The cross section, $\langle \sigma(E_{\text{c.m.}}) \rangle = \frac{\int \sigma(E)dE}{\int dE}$, averaged over the target energy width ($E_{\text{c.m.}} - \Delta \frac{E_T}{2} < E < E_{\text{c.m.}} + \Delta \frac{E_T}{2}$) is first calculated at each $E_{\text{c.m.}}$ by using the well known energy dependence of σ that arises mostly from the Coulomb barrier penetrability effect [see Eq. (2) below]. The $S(E)$ from Ref. [25] is used to obtain $\sigma(E)$. The effective energies, $\overline{E}_{\text{c.m.}}$, are then computed by solving $\langle \sigma(E_{\text{c.m.}}) \rangle = \sigma(\overline{E}_{\text{c.m.}})$. To estimate the energy averaging effect $E_{\text{c.m.}}$ (Table I) and the corresponding $\overline{E}_{\text{c.m.}}$ can be compared, and negligible differences are found. For example, at $E_{\text{c.m.}} = 420$ keV where a maximum averaging effect is expected, only a difference of $\sim 0.1\%$ (0.3 keV) is found. A different parametrization of $S(E)$ from Ref. [26] is also tried, and no significant change in averaging effects is found. The target length l and ^4He gas pressure P are

accordingly adjusted for each of the beam energies to obtain ΔE_{He} that gives a negligible averaging effect but a high ^7Be production yield. ^7Be decays to the 478 keV state in ^7Li with $T_{1/2} = 53.29(7)$ days [27] and a branching ratio of 10.52(6)% [28]. The number of ^7Be nuclei is determined by measuring the ^7Be activity on a Cu catcher at Soreq Research Centre using a Ge detector setup, similar to that used in the precision determination of the ^7Be target strength for the S_{17} measurement [5]. To cover a large solid angle, the Cu catcher was placed at a distance of 20 mm from a HPGe detector that was shielded from room background; the activity was measured over a period of 3 to 6 days. A ^7Be reference point source of 2 mm diameter with a precisely known γ-ray emission rate [5] was used for the efficiency calibration at 478 keV. The ^7Be products subscribe to an approximately 20 mm diameter spot (TRIM [23]), still much smaller than the catcher's diameter, and a correction factor of 1.3% to the detection efficiency due to an extended source had to be determined by measuring the count rate of the reference point source at off-center locations. The resulting overall detection efficiency at this geometry was determined to be 0.0436(5) at 478 keV. The ambient background was monitored periodically, and a typical spectrum accumulated over ~ 4 days is shown in Fig. 2, demonstrating that there is no interfering peak around 478 keV. A Cu catcher bombarded with a ^3He beam, but no ^4He gas showed no 478 keV peak. γ spectra measured with Cu catchers prepared at $E_{\text{c.m.}} = 420$ and 950 keV are shown in Fig. 2. The number of ^7Be nuclei $N_{^7\text{Be}}(0)$ is obtained from the efficiency corrected 478 keV γ yield and the known branching ratio and half-life. For example, for $E_{\text{c.m.}} = 420$ keV, the net peak area, the activity, and the number of ^7Be atoms were 898 (54) counts, 0.389 (24) Bq, and 2.59 (16) $\times 10^6$ atoms, respectively, including uncertainties of detection efficiency from the

TABLE I. Capture cross sections at different values of $E_{\text{c.m.}}$, Ni windows, target gas pressure (P), and length (l). σ^R and σ: The cross sections values obtained by using the number of beam particles from Rutherford scattering and charge integration, respectively. $S(E)$: S factors corresponding to σ. The errors due to statistics (activity measurements) and systematics (P, T_c and $E_{\text{c.m.}}$) are also given in separate brackets. The latter errors on $S(E)$ include also the uncertainties on energy losses and straggling (see text).

| $E_{\text{c.m.}}$ (keV)	Ni (μm)	P (torr)	l (cm)	σ^R (nb)	σ (nb)	$S(E)$ (keV b)
951.0	1.00	50.0	10.33	1680(59)(37)	1680(59)(29)	0.328(12)(7)
951.0	1.00	36.8	13.66	1500(45)(33)	1530(46)(26)	0.299(8)(7)
951.0	1.00	34.9	13.93	1830(75)(40)	1720(71)(29)	0.335(14)(9)
951.0	1.00	52.8	10.35	1700(76)(37)	1600(72)(27)	0.312(14)(8)
950.0	0.50	51.3	10.35	1580(57)(35)	1690(61)(29)	0.330(12)(9)
950.0	1.00	50.4	10.35	1518(58)(33)	1586(61)(27)	0.309(12)(8)
$\overline{9}50.0$	$\cdots$	$\cdots$	$\cdots$	1620(31)(37)	1620(31)(29)	0.316(6)(7)
624.0	1.00	50.0	10.35	764(30)(17)	794(31)(14)	0.353(14)(17)
605.0	0.50	50.0	10.35	767(31)(17)	777(31)(13)	0.372(15)(15)
$\overline{6}14.5$	$\cdots$	$\cdots$	$\cdots$	766(22)(17)	786(22)(13)	0.362(10)(15)
506.0	0.75	22.4	10.35	476(16)(10)	508(17)(8)	0.379(15)(27)
420.0	1.00	20.4	10.35	303(9)(7)	333(10)(6)	0.420(14)(30)
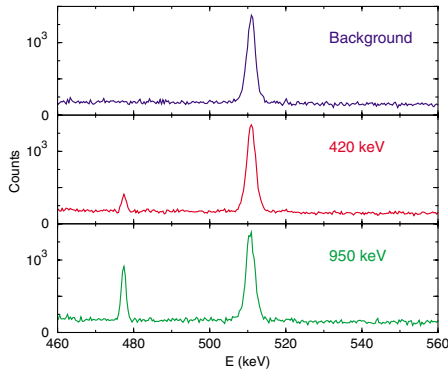
FIG. 2 (color online). γ spectra from ambient background and from the Cu catchers of $E_{c.m.} = 420$ and 950 keV. The spectra are normalized to the background 511 keV, the only visible γ line in this energy range besides the 478 keV from ^{7}Be.

^{7}Be reference source, counting geometry, and radial distribution of the ^{7}Be on the Cu catcher. The number of beam particles N_p obtained through either the beam current integration or the Rutherford scattering from the nickel foil is the other major source of error in the determination of the cross section. For the scattered flux measurement ($\sim 1.8\%$), the sources of error include (a) θ ($< 0.5\%$) and $d\Omega$ (1.1%) of the Si monitor detector. θ was cross-checked using the elastic scattering at different energies of ^{4}He beam from ^{12}C foil. For $d\Omega$ determination, the diameter of the collimator used on the particle detector was measured using an α source as ≈ 0.217 mm relative to a mechanically well measurable reference collimator of diameter 4 mm. (b) Ni-foil thickness (2%) was measured by weighing and from alpha particle energy losses. These were cross-checked with width measurements using an electron microscope. The errors in $E_{c.m.}$, resulting mainly from the Ni-foil thickness, were determined for each measurement (Table I) from the peak position and width of the scattered-beam spectra, with and without gas (E_b) and by using TRIM calculations (ΔE_{Ni}, ΔE_{He}) (1.5%).

Other sources of error include (1) gas pressure ($< 0.5\%$), (2) bowing effect on the gas cell length resulting from the pressure difference between the beam line and the chamber ($< 0.5\%$), (3) T_c ($< 1.0\%$), and (4) current integration ($\sim 1.2\%$). The current integration and the scattered particles were compared continuously and were found to be stable within a mean deviation of 1.2%. These errors were of similar magnitude for all our measurements, yielding a total error of 1.7%. In Table I we present the cross sections obtained utilizing both current integration (1.7%), σ, as well as the Rutherford scattering (2.2%), σ^R. As evident from Table I, the extracted values obtained from both σ^R and σ show no major differences, and the latter is used, with negligible consequences on the extracted final result for $S_{34}(0)$.

The measurements were carried out at $E_{c.m.} = 420$, 506, 605, 624, and ≈ 950 keV. ==The latter energy point was== ==remeasured several times by varying experimental parameters such as ^{4}He gas pressure, beam current, and Ni-foil thicknesses, yielding consistent values (Table I).==

The astrophysical $S(E)$ factor is related to the cross section $\sigma(E)$ by

$$S(E) = E\sigma(E) \exp(2\pi\eta), \qquad (2)$$

where $2\pi\eta = 164.12/E^{1/2}$ and E is given in keV. Table I presents measured cross sections and extracted S factors at various $E_{c.m.}$. To examine the issue of the absolute scale of various measurements, we have carried out a χ^2 compatibility analysis between $S(E)$ values from previous data sets (grouped together in the vicinity of the present energies) and the present data (Table II). The results of Hilgemeier *et al.* [10] are in best agreement with ours, while other data sets exhibit a varying degree of difference and scatter. It should be noted that the analysis is somewhat limited due to the availability of the data points around the energies of the present work.

The various theoretical models [18,25,26,29–32] are normally constrained by nuclear model parameters that reproduce measured nuclear properties such as binding energies, branching ratios, charge radii, and electric quadrupole moments and largely yield a similar energy dependence of the $S(E)$ factor. Because of remaining ambiguities, the overall normalization is left as a free parameter to be fitted to the data, subject to the constraint: $0.4 \leq S(0) \leq 0.9$ keV b [25]. These fits (Fig. 3) yield extrapolated values of $S_{34} = 0.53(2)(1)$ and $0.53(3)(1)$ keV b for the present data alone and when combined with the data from Ref. [10], respectively. The errors in brackets represent the experimental error and the variation of the extrapolated $S_{34}(0)$ using a particular theory, respectively. The experimental error includes $\sim 0.7\%$ uncertainty due to the error in $E_{c.m.}$ resulting from air contamination. It is also instructive to include the extensive data set from Ref. [15] that exhibits a similar energy dependence of $S(E)$, in the fit to the present results, with the addition of an interset normalization parameter, yielding $S_{34} = 0.53(3)(1)$ keV b. The excellent agreement of the present values with the prompt-γ

TABLE II. A χ^2 comparison of S factors from the present data and from former measurements, interpolated using two or more neighboring data points to correspond to the energies of the current experiment. The $S_{34}(E)$ from Ref. [15] have been scaled up by 40%, as suggested in Ref. [10]. The data from Ref. [11] include both prompt γ and ^{7}Be activity measurements.

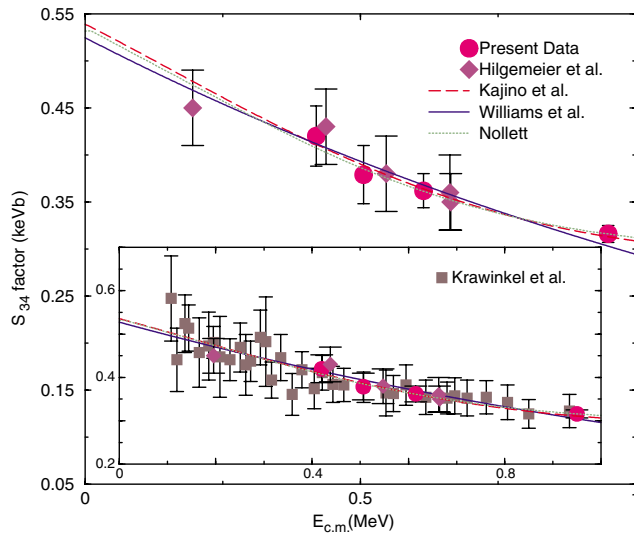| $E_{c.m.}$ (keV)	Present	[15]	[10]	[11]	[13,14]
420.0	0.420(32)	0.38(2)	0.44(4)	0.38(1)	0.42(2)
506.0	0.379(31)	0.36(1)	0.40(4)	0.39(1)	0.35(2)
615.0	0.362(18)	0.34(2)	0.36(4)	0.40(1)	0.37(2)
950.0	0.316(9)	0.30(2)	0.28(4)	0.36(2)	0.26(1)
χ^2	$\cdots$	2.7	1.1	9.0	18.0

FIG. 3 (color online). Present data together with that of Ref. [10] and representative theoretical fits, yielding $S_{34}(0) = 0.533(20)(7)$ keV b. Inset: the results of renormalized Ref. [15] (see text) are also included to yield $0.532(30)(4)$ keV b.

values of Ref. [10] and with the renormalized data of Ref. [15] results in a statistical agreement between prompt-γ and decay-γ measurements [18]. The procedures outlined above are all consistent, and we quote a final recommended result of $S_{34} = 0.53(2)(1)$ keV b.

The $S_{34}(0)$ value used in the current SSM [2] yields a 8% uncertainty in the predictions of both the ^{7}Be and ^{8}B neutrino fluxes. Since these fluxes are proportional to $S_{34}^{0.86}(0)$ and $S_{34}^{0.81}(0)$, respectively [33], the current result of $S_{34}(0) = 0.53(2)(1)$ keV b brings down the uncertainty to a level of 5%. The quoted value of $S_{34}(0)$ also provides a more accurate and reliable input for the SBBN simulations. The present recommended value is in excellent agreement with $0.51(4)$ keV b of the most recent R matrix analysis [21]. We note that the agreement with [21] is even more remarkable if one applies the renormalization to the data of [15] as outlined above. The present value highlights the issue of the marked discrepancy between the calculated ^{7}Li abundance using the baryon density from cosmic microwave radiation measurements and observations [20] and emphasizes the need for another resolution to this discrepancy.

[1] J. N. Bahcall *et al.*, Astrophys. J. **555**, 990 (2001).
[2] J. N. Bahcall and M. H. Pinsonneault, Phys. Rev. Lett. **92**, 121301 (2004).
[3] S. Fukuda *et al.*, Phys. Rev. Lett. **86**, 5656 (2001).
[4] Q. R. Ahmad *et al.*, Phys. Rev. Lett. **89**, 011301 (2002).
[5] L. T. Baby *et al.*, Phys. Rev. Lett. **90**, 022501 (2003); Phys. Rev. C **67**, 065805 (2003).
[6] A. R. Junghans *et al.*, Phys. Rev. Lett. **88**, 041101 (2002); Phys. Rev. C **68**, 065803 (2003).
[7] F. Schumann *et al.*, Phys. Rev. Lett. **90**, 232501 (2003).
[8] Kenneth M. Nollett Phys. Rev. C **63**, 054002 (2001).
[9] Richard H. Cyburt *et al.*, Phys. Rev. D **69**, 123519 (2004).
[10] M. Hilgemeier *et al.*, Z. Phys. A **329**, 243 (1988).
[11] J. L. Osborne *et al.*, Nucl. Phys. **A419**, 115 (1984).
[12] T. K. Alexander *et al.*, Nucl. Phys. **A427**, 526 (1984).
[13] P. D. Parker *et al.*, Phys. Rev. **131**, 2578 (1963).
[14] K. Nagatani *et al.*, Nucl. Phys. **A128**, 325 (1969).
[15] H. Krawinkel *et al.*, Z. Phys. A **304**, 307 (1982).
[16] R. G. H. Robertson *et al.*, Phys. Rev. C **27**, 11 (1983).
[17] H. Volk *et al.*, Z. Phys. A **310**, 91 (1983).
[18] E. Adelberger *et al.*, Rev. Mod. Phys. **70**, 1265 (1998).
[19] C. Angulo *et al.*, Nucl. Phys. **A656**, 3 (1999).
[20] A. Coc *et al.*, Astrophys. J. **600**, 544 (2004).
[21] P. Descouvemont *et al.*, At. Data Nucl. Data Tables **88**, 203 (2004).
[22] J. Gorres *et al.*, Nucl. Instrum. Methods Phys. Res., Sect. A **241**, 334 (1985).
[23] SRIM 2003 package from www.srim.org.
[24] L. Weissmann *et al.*, Nucl. Phys. **A630**, 678 (1998).
[25] T. Kajino *et al.*, Astrophys. J. **319**, 531 (1987); Nucl. Phys. **A460**, 559 (1986).
[26] R. D. Williams *et al.*, Phys. Rev. C **23**, 2773 (1981).
[27] Nuclear Wallet Cards, edited by J. K. Tuli (National Nuclear Data Center, Upton, NY, 2000), 6th ed.
[28] See S. Y. F. Chu, L. P. Ekstrom, and R. B. Firestone, nucleardata.nuclear.lu.se/nucleardata/toi/.
[29] T. A. Tombrello *et al.*, Phys. Rev. **131**, 2582 (1963).
[30] Q. K. K. Liu *et al.* Phys. Rev. C **23**, 645 (1981).
[31] B. T. Kim *et al.*, Phys. Rev. C **23**, 33 (1981).
[32] A. Csótó and K. Langanke, Few Body Systems **29**, 121 (2000).
[33] J. N. Bahcall and R. Ulrich, Rev. Mod. Phys. **60**, 297 (1988).